Supplementary figure 1

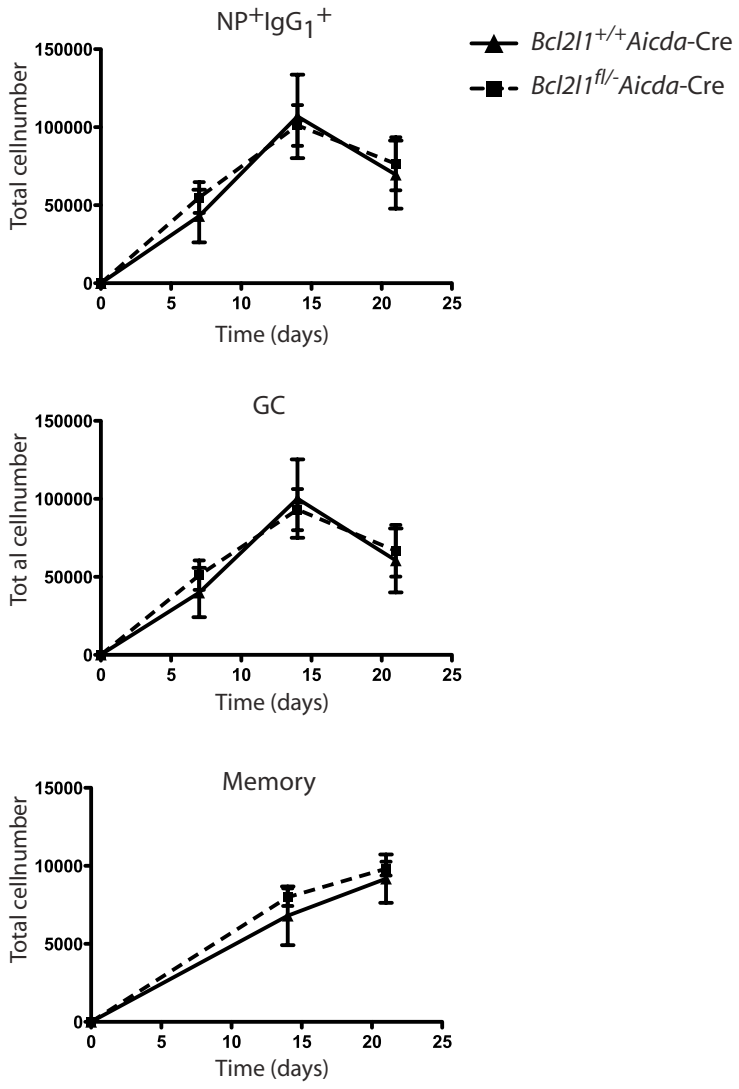


**Fig. S1.** Kinetics of the GC response in *Bcl2l1* deficient mice.
Flow cytometric analysis of splenocytes on days 7, 14 and 21 after intraperitoneal immunization with NP-KLH in alum. Isotype switched ($IgM^-IgD^-Gr\text{-}1^-CD138^-B220^+$) B cells were analysed for $NP^+IgG_1{}^+$ status and then sub-divided into GC ($CD38^-$) and memory ($CD38^+$) B cells. Numbers of each of the respective populations (total, GC and memory) are plotted. Data are the mean ± SEM of between three and six mice in each group and summarize two experiments for each time point. One experiment used mice reconstituted with *Bcl2l1*$^{fl/-}$*Aicda*-Cre or *Bcl2l1*$^{+/+}$*Aicda*-Cre bone marrow.

Supplementary figure 2

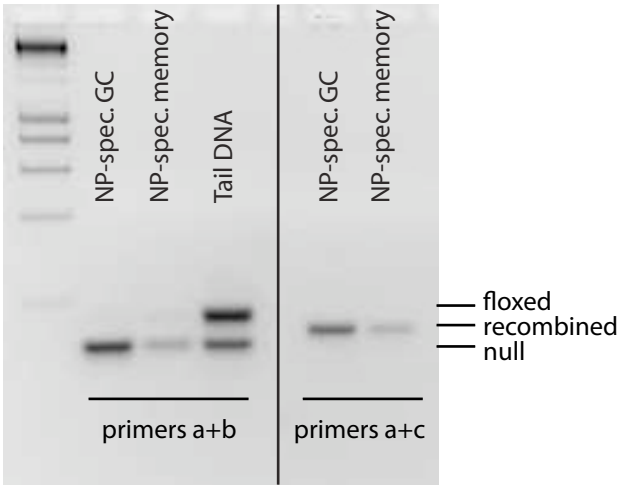


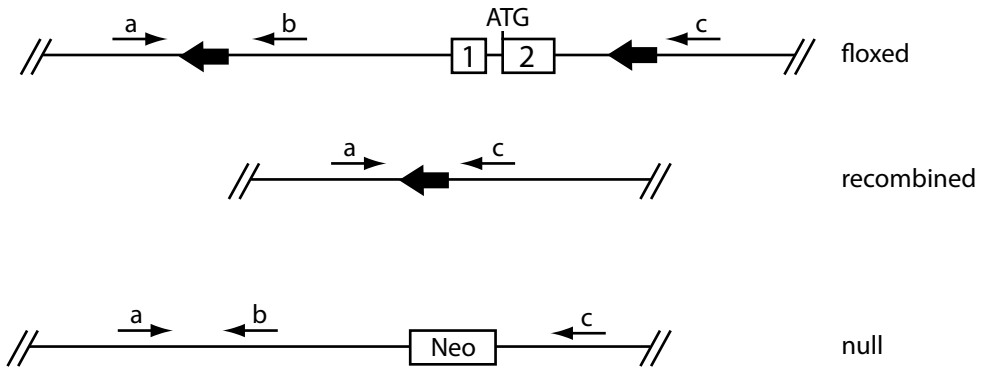


**Fig. S2.** The *Bcl2l1* floxed allele is efficiently deleted in *Bcl2l1*$^{fl/-}$*Aicda*-Cre GC and memory B cells. PCR detecting the floxed and deleted *Bcl2l1* alleles in DNA from sorted GC ($NP^+IgG_1{}^+CD38^-$) and memory ($NP^+IgG_1{}^+CD38^+$) B cells from two *Bcl2l1*$^{fl/-}$*Aicda*-Cre immunized mice, as well as in tail DNA from a *Bcl2l1*$^{fl/-}$*Aicda*-Cre mouse. Empty lanes from a single gel were removed from the image, rejoining indicated by the solid line. The data are representative of two independent experiments. Lower panel is a schematic representation of the *Bcl2l1* alleles used in these experiments. The floxed allele, before and after Cre-mediated deletion, and the null allele are shown. The positions where PCR primers bind are also indicated.

Supplementary figure 3

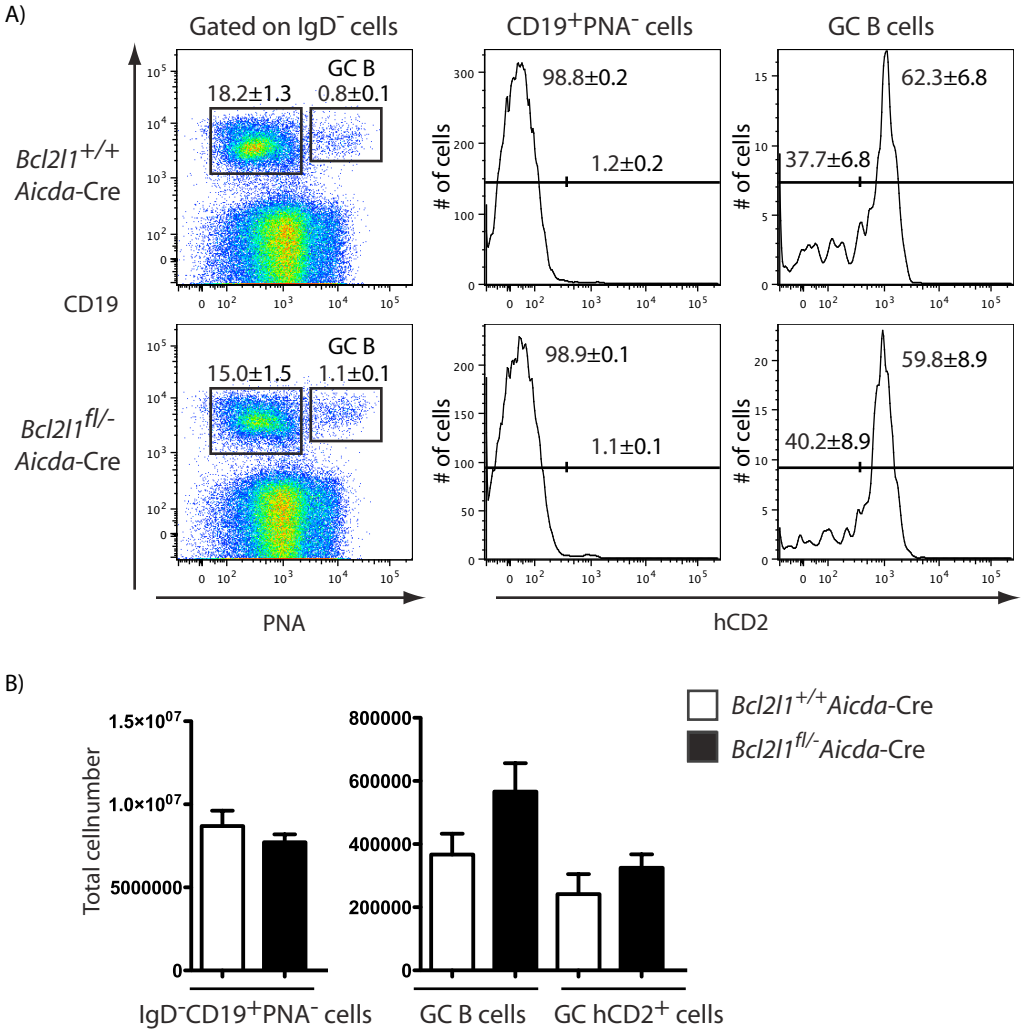


**Fig. S3.** Expression of *Aicda* and Cre recombinase in GC B cells but not follicular B cells in *Bcl2l1*$^{fl/-}$*Aicda* -Cre mice.
(**A**) Flow cytometric analysis of splenocytes 21 days after intraperitoneal immunization with NP-KLH in alum. Non-GC (IgD$^-$CD19$^+$PNA$^-$) and GC (IgD$^-$CD19$^+$PNA$^+$) B cells were analysed for levels of hCD2t indicating expression of *Aicda* and Cre recombinase. Numbers in dot plots and histograms are mean percentage ± SEM. (**B**) Total cell numbers of the populations identified in (A) are plotted as the mean ± SEM of between four and six mice in each group, summarizing two experiments.

Supplementary figure 4

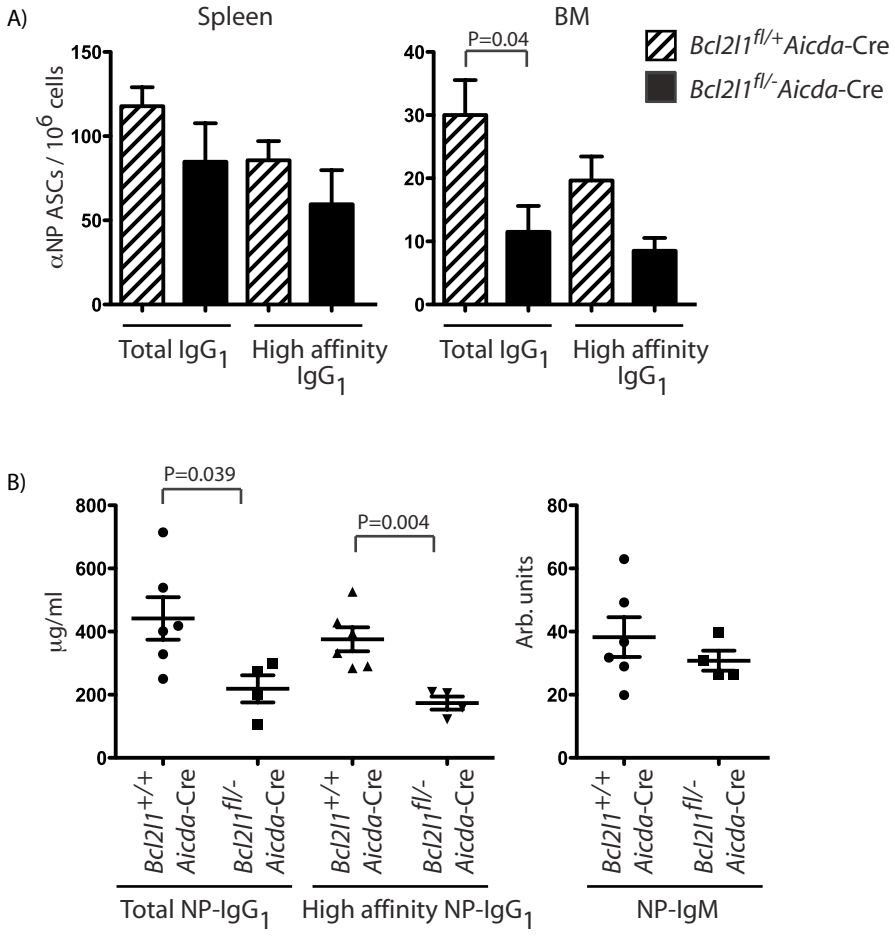


**Fig. S4**. *Bcl2l1* contributes to the survival of emigrating plasma cells and antibody titres.
(**A**) Frequencies of total and high affinity NP-specific $IgG_1$-secreting antibody secreting cells in spleen and bone marrow 14 days after intraperitoneal immunization of *Bcl2l1* conditionally targeted mice with NP-KLH in alum. Data are the mean ± SEM of replicate wells with four to six mice in each group and summarize two experiments. (**B**) ELISA of total (NP13) and high affinity (NP2) anti-NP-$IgG_1$ and total anti-NP-IgM in serum, measured on day 21 after immunization. Values from individual mice are shown, as are the means ± SEM. Significant differences in (A) and (B), determined by Student's T-test, are shown.

Supplementary figure 5

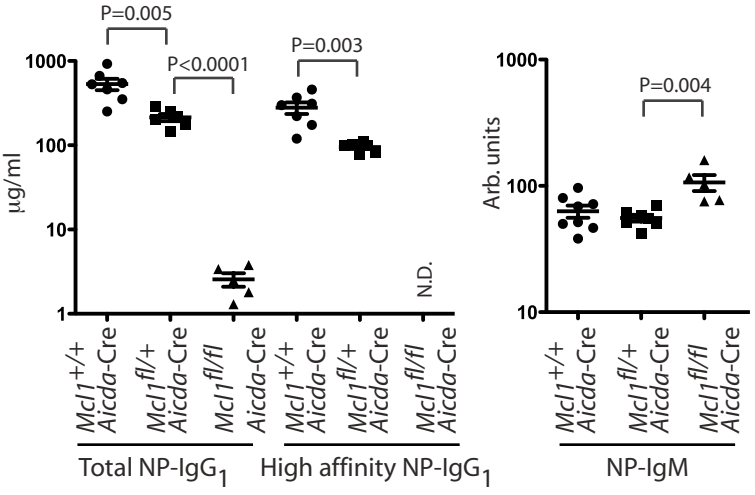


**Fig. S5**. Conditional deletion of *Mcl1* abrogates the formation of NP-specific plasma cells.
ELISA of total (NP13) and high affinity (NP2) anti-NP-$IgG_1$ and total anti-NP-IgM in serum, measured on day 14 after intraperitoneal immunization with NP-KLH in alum. Data are the mean ± SEM of between five and eight mice in each group and summarize three experiments. Values from individual mice are shown, as are the means ± SEM. Significant differences, determined by Student's T-test, are shown.

Supplementary figure 6

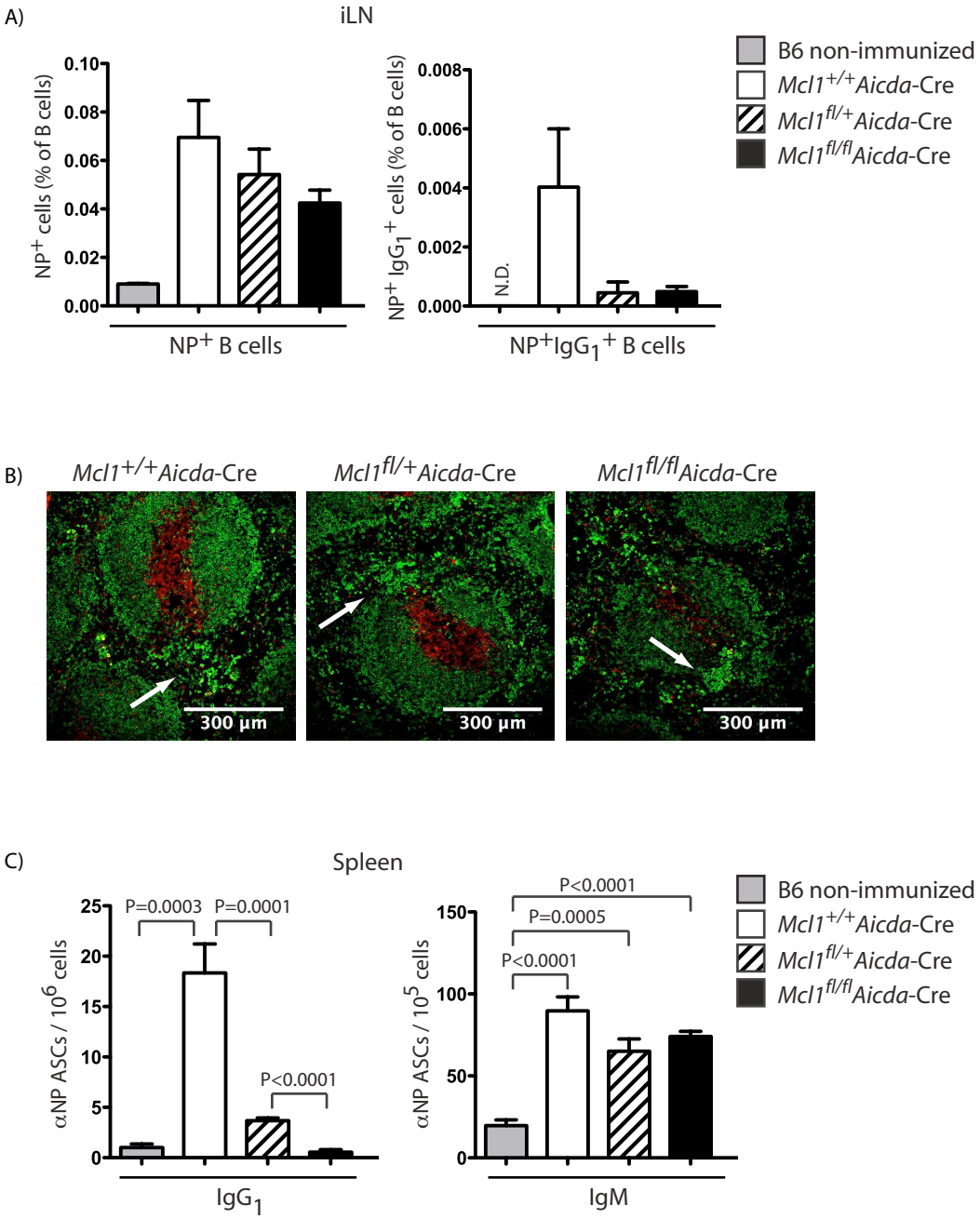


**Fig. S6**. Loss of *Mcl1* blocks appearance of $NP^+IgG_1^+$ B cells on day 5 of the immune response. (**A**) Frequency of NP-binding (left) and $NP^+IgG_1^+$ (right) B cells in inguinal lymph nodes (iLN) 5 days after subcutaneous immunization of mice with NP-KLH in alum. Status of the *Mcl1* locus and *Aicda*-Cre are indicated. All immunized mice show an expansion of NP-reactive B cells, but loss of *Mcl1* coincident with expression of AID prevents appearance of $NP^+IgG_1^+$ cells. B6 are non-immunized C57BL/6 controls. (**B**) Frozen sections of spleens from the indicated strains 5 days after immunization, stained with anti-IgM (green) and anti-CD3 (red). Foci of IgM ASC developed in the bridging channels in all strains, indicated by arrows. Original magnification x 20 with scale indicated. (**C**) ELISPOT analysis of NP-reactive ASC in spleens 5 days after immunization showing equal development of IgM ASC (right) but deficiency of $IgG_1$ ASC in strains capable of deleting *Mcl1*. Significant differences, calculated using Student's T-test, are indicated. Data are from 3 mice per group.

Supplementary figure 7

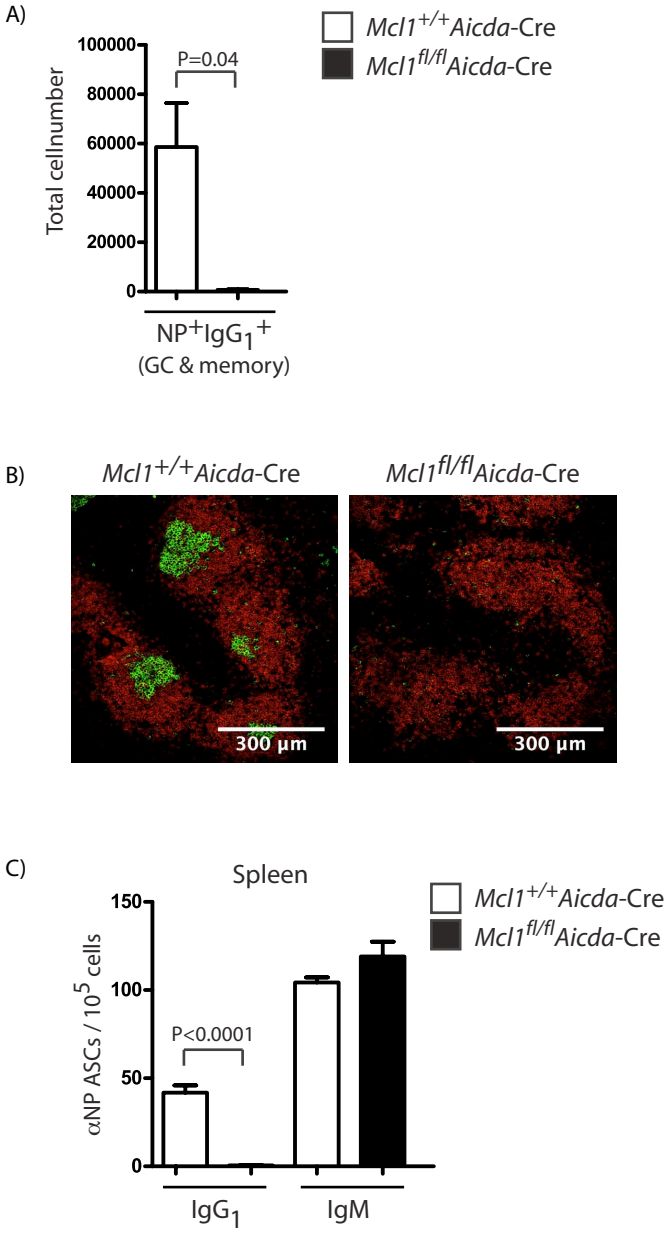


**Fig. S7**. Loss of *Mcl1* blocks appearance of $NP^+IgG_1^+$ B cells on day 7 of the immune response
(**A**) Absolute number of $NP^+IgG_1^+$ B cells in the spleens of mice immunized by intraperitoneal injection of NP-KLH in alum 7 days previously. Status of the *Mcl1* locus and *Aicda*-Cre are indicated. Significant differences, calculated using Student's T-test, are indicated. (**B**) Frozen sections of spleens from the indicated strains 7 days after immunization, stained with anti-B220 (red) and anti-GL7 (green). GC are not apparent in *Mcl1*$^{fl/fl}$*Aicda*-Cre mice. Original magnification x 20 with scale indicated. (**C**) ELISPOT analysis of NP-reactive ASC in spleens 7 days after immunization showing equal development of IgM ASC but deficiency of $IgG_1$ ASC in mice capable of deleting *Mcl1*. Significant differences, calculated using Student's T-test, are indicated. Data are from 4 mice per group.

Supplementary figure 8

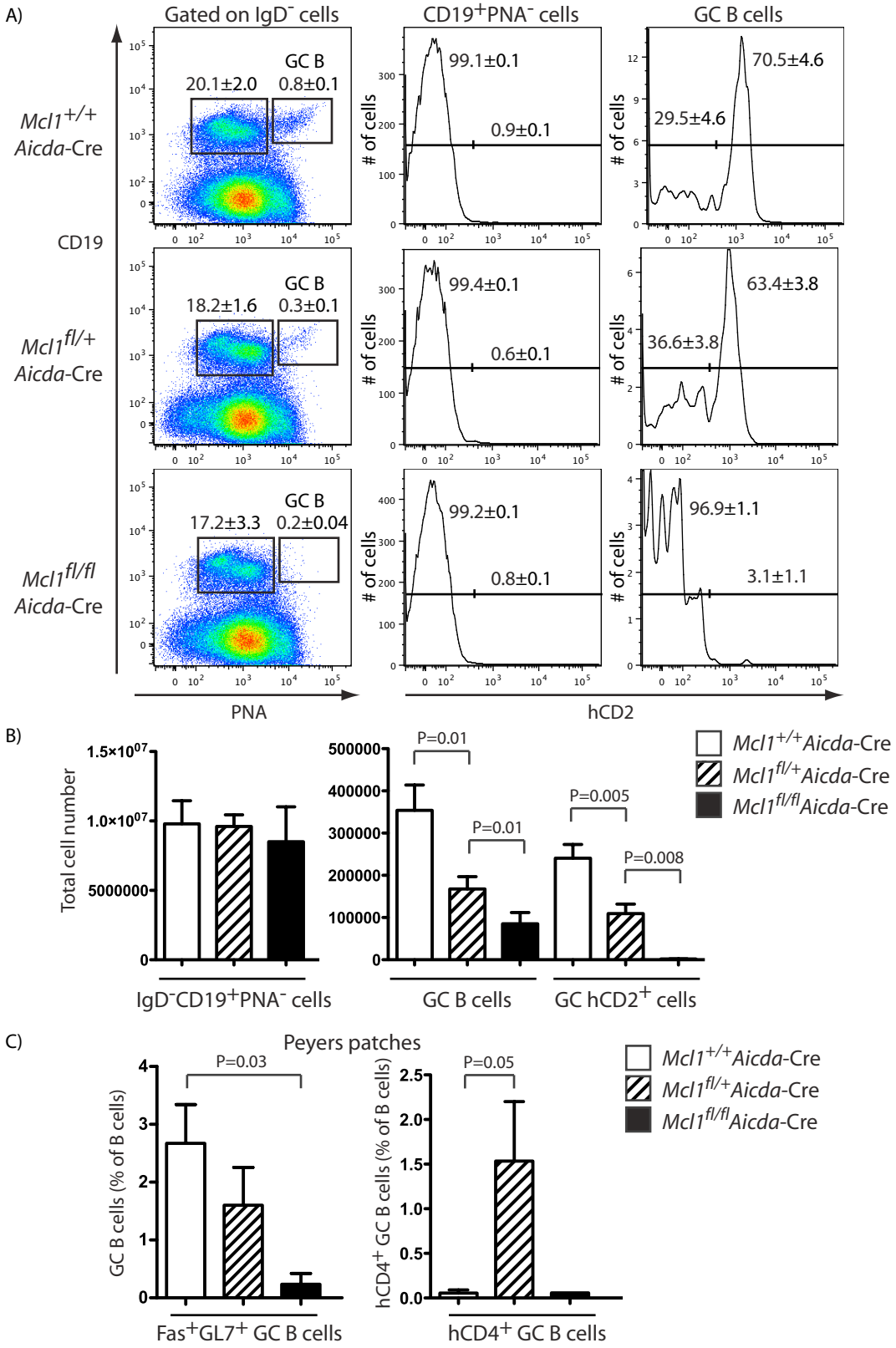


**Fig. S8.** Deletion of GC B cells expressing *Aicda* and Cre recombinase in *Mcl1*$^{fl/fl}$*Aicda* -Cre mice. (**A**) Flow cytometric analysis of splenocytes 14 days after intraperitoneal immunization with NP-KLH in alum. Non-GC (IgD$^-$CD19$^+$PNA$^-$) and GC (IgD$^-$CD19$^+$PNA$^+$) B cells were analysed for *hCD2t* expression, indicating co-expression of *Aicda* and Cre recombinase. Numbers in plots and histograms are the mean percentages ± SEM. (**B**) Total cell numbers of the populations identified in (A) are graphed as the mean ± SEM of between four and eight mice in each group, summarizing three experiments. (**C**) Peyer's patches, collected from the indicated groups of mice, were analysed for the representation of GC B cells (CD19$^+$FAS$^+$GL7$^+$) amongst all B cells (left) and of hCD4$^+$ GC B cells (right). Significant differences, calculated using Student's T-test, are indicated. Data arefrom 3-4 mice per group.

Supplementary figure 9

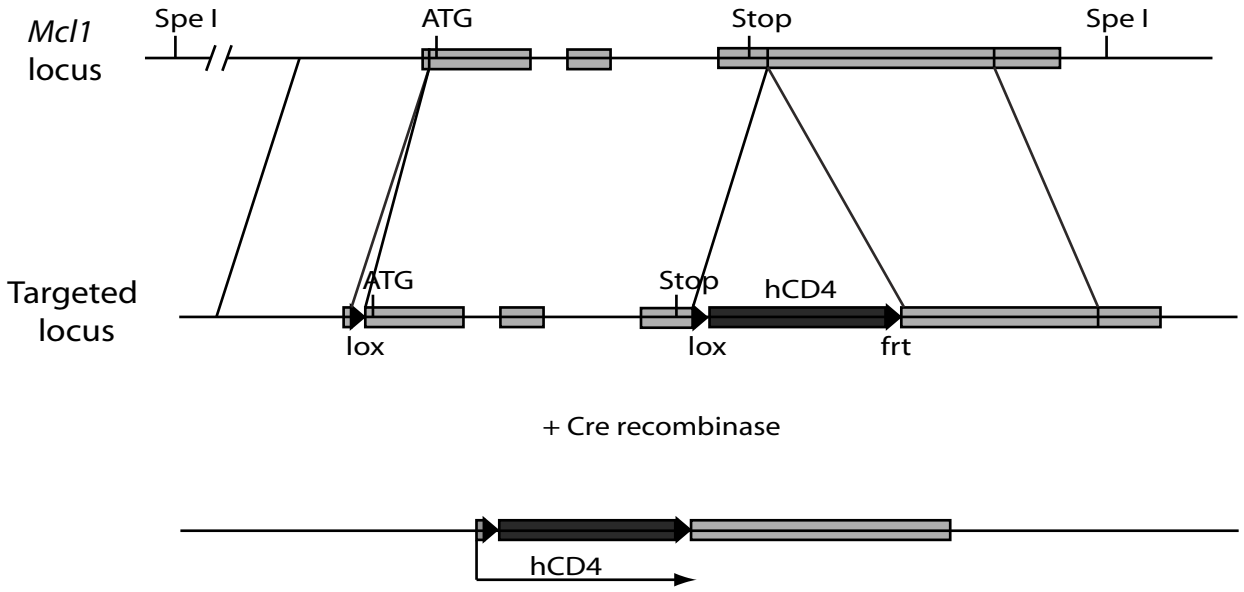


**Fig. S9.** *Mcl1* gene-targeting construct
The construct designed to introduce LoxP sites flanking the *Mcl1* locus contains *hCD4* such that upon *Mcl1* deletion, it is subjugated to the promoter of *Mcl1*. hCD4 is subsequently expressed on the cell surface serving as a reporter for both deletion of the *Mcl1* allele and *Mcl1* transcription.

Supplementary figure 10

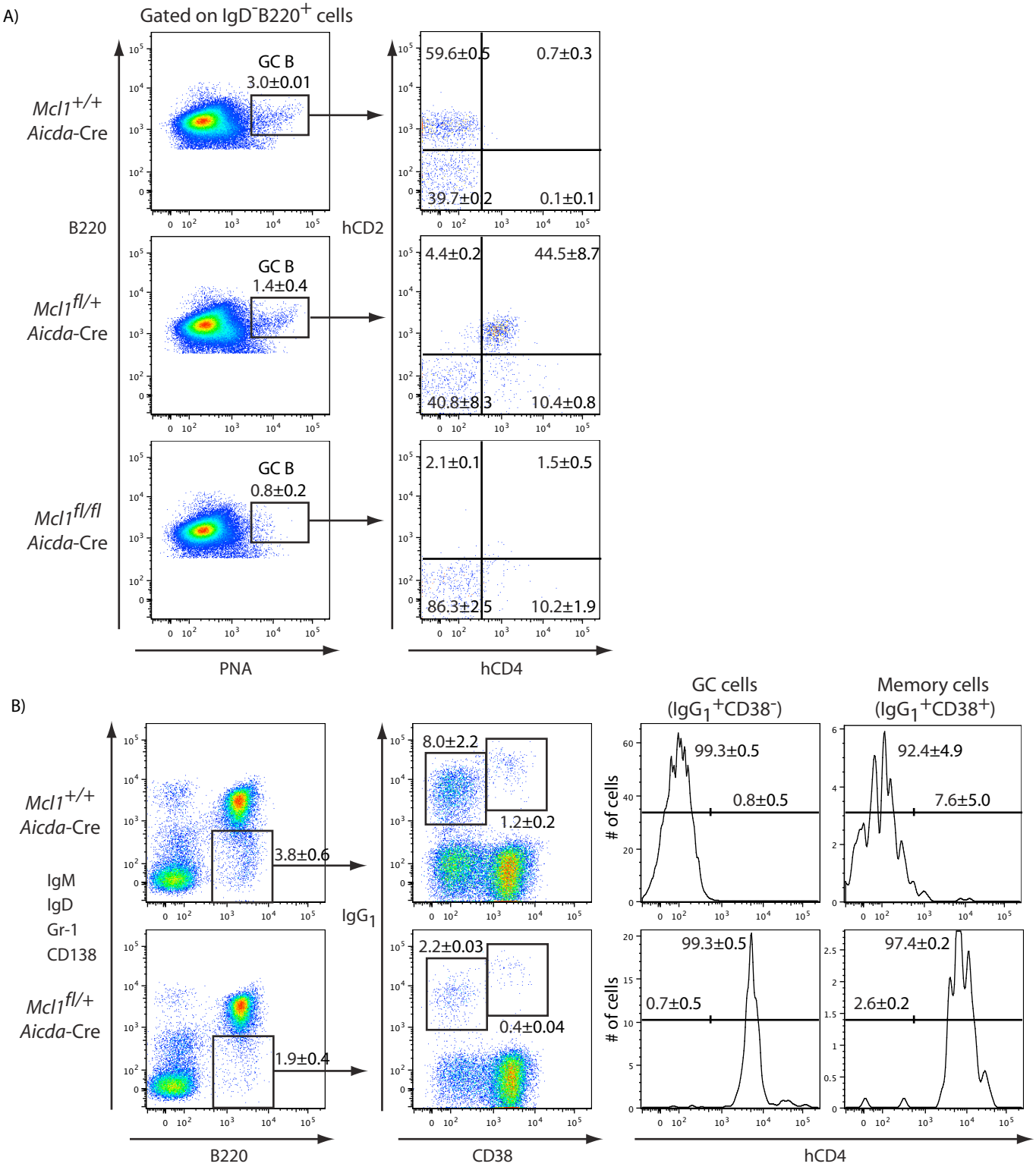


**Fig. S10.** *Mcl1* is efficiently deleted in GC and memory B cells as reported by *hCD4* expression. (**A**) Flow cytometric analysis of splenocytes 14 days after intraperitoneal immunization with NP-KLH in alum. GC ($IgD^-B220^+PNA^+$) B cells were analysed for *hCD2t*, reporting co-expression of *Aicda* and Cre recombinase as well as amounts of *hCD4*, reporting *Mcl1* deletion. Numbers in plots are the mean percentages ± SEM. Data are the means ± SEM of two or three mice in each group. (**B**) $IgG_1^+$ GC B cells ($CD38^-$) and memory B cells ($CD38^+$) in $Mcl1^{fl/+}$*Aicda*-Cre mice were assessed for *hCD4* expression. Numbers in dotplots and histograms are mean percentages ± SEM of at least two mice in each group.

Supplementary figure 11

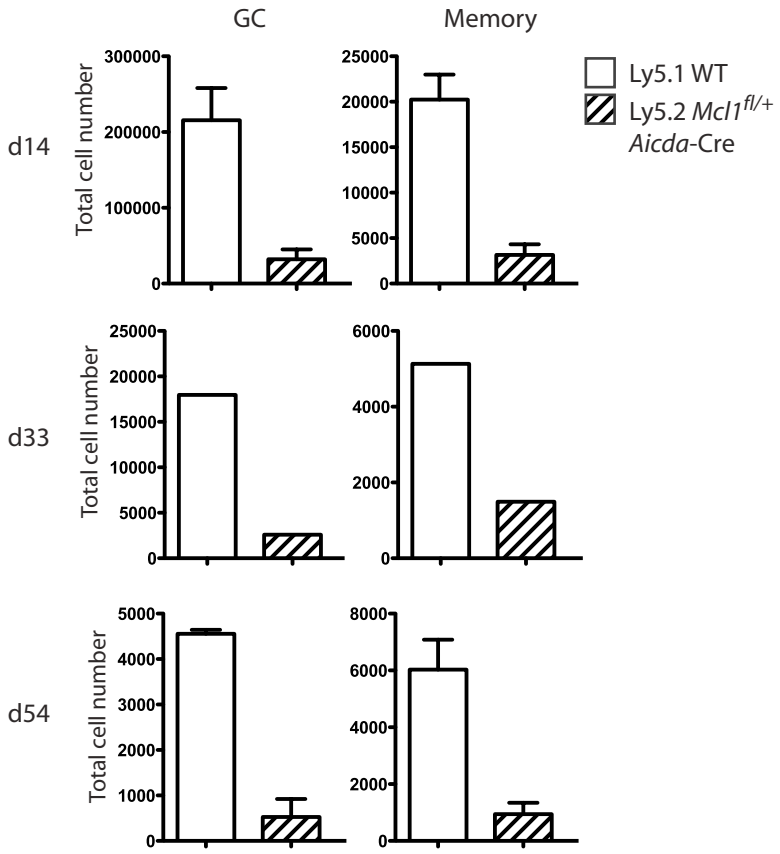


**Fig. S11.** Comparable fold reduction of *Mcl1*$^{fl/+}$ B cells amongst the GC and memory compartments that remain constant over time.
Absolute numbers of $NP^{+}IgG_1{}^{+}$ GC ($CD38^{-}$) and memory B cells ($CD38^{+}$) arising from each genotype in *Mcl1*$^{fl/+}$*Aicda*-Cre/Ly5.1 chimeras at 14, 33 and 54 days after intraperitoneal immunization with NP-KLH in alum are graphed as the mean ± SEM of between 2 and 3 mice for each time point.

Supplementary figure 12

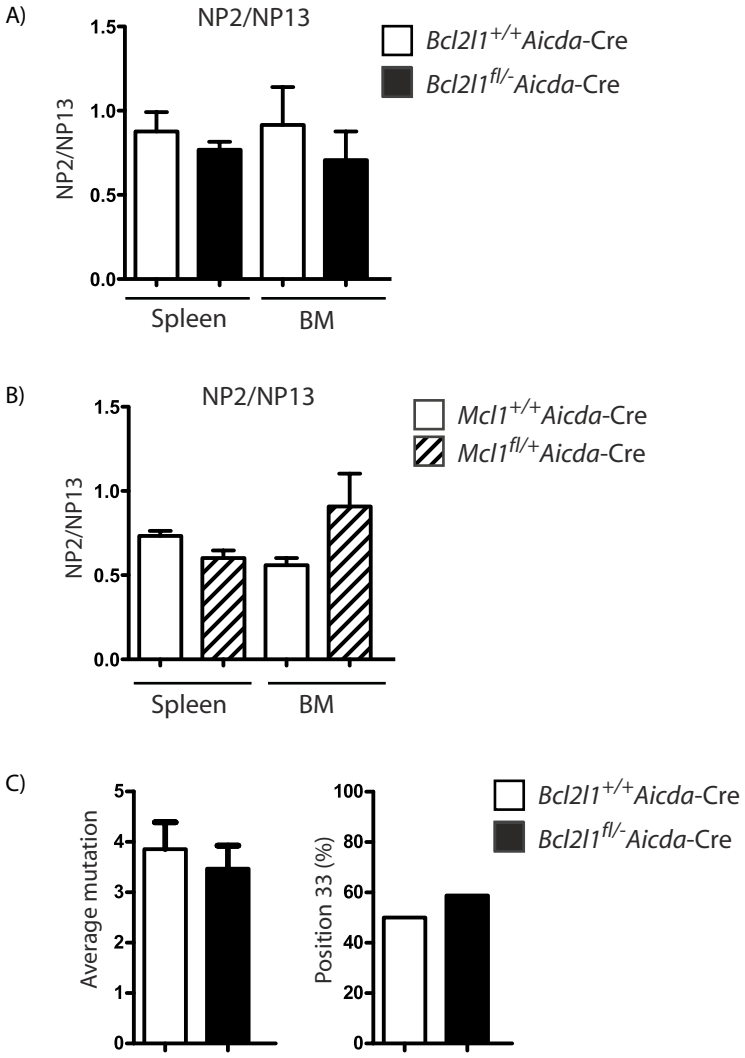


**Fig. S12.** Affinity maturation amongst NP-reactive B cells is unaffected by loss of either *Bcl2l1* or *Mcl1*. (**A**) Affinity maturation of NP-specific $IgG_1$ ASCs calculated as a ratio of NP2/NP13 for mice of the indicated genotypes on day 21 post immunization. Data are the mean ± SEM from 4 – 6 mice per group with tissues and configuration of the *Bcl2l1* and *Aicda*-Cre alleles indicated. (**B**) Affinity maturation of NP-specific $IgG_1$ ASCs calculated as a ratio of NP2/NP13 for mice of the indicated genotypes on day 21 post immunization. Data are the mean ± SEM from 5 - 10 mice per group with tissues and configuration of the *Mcl1* and *Aicda*-Cre alleles indicated. (**C**) Analysis of somatic hypermutation amongst $NP^+IgG_1{}^+CD38^{hi}$ memory B cells from mice of the indicated *Bcl2l1* genotypes assessed by comparing point mutations in the $V_H186.2$ genes of single antigen specific B cells sorted 21 days after immunization with those in controls. Average mutation indicates the average number of point mutations per $V_H186.2$ gene segment determined by comparing the region encoding amino acids 10 to 96 with the germline sequence from 17 *Bcl2l1* deleted cells with 14 controls. Position 33 (%) measures the frequency of the Trp to Leu exchange within CDR1 of $V_H186.2$ that alone confers a 10-fold increase in affinity of binding NP.

Supplementary figure 13

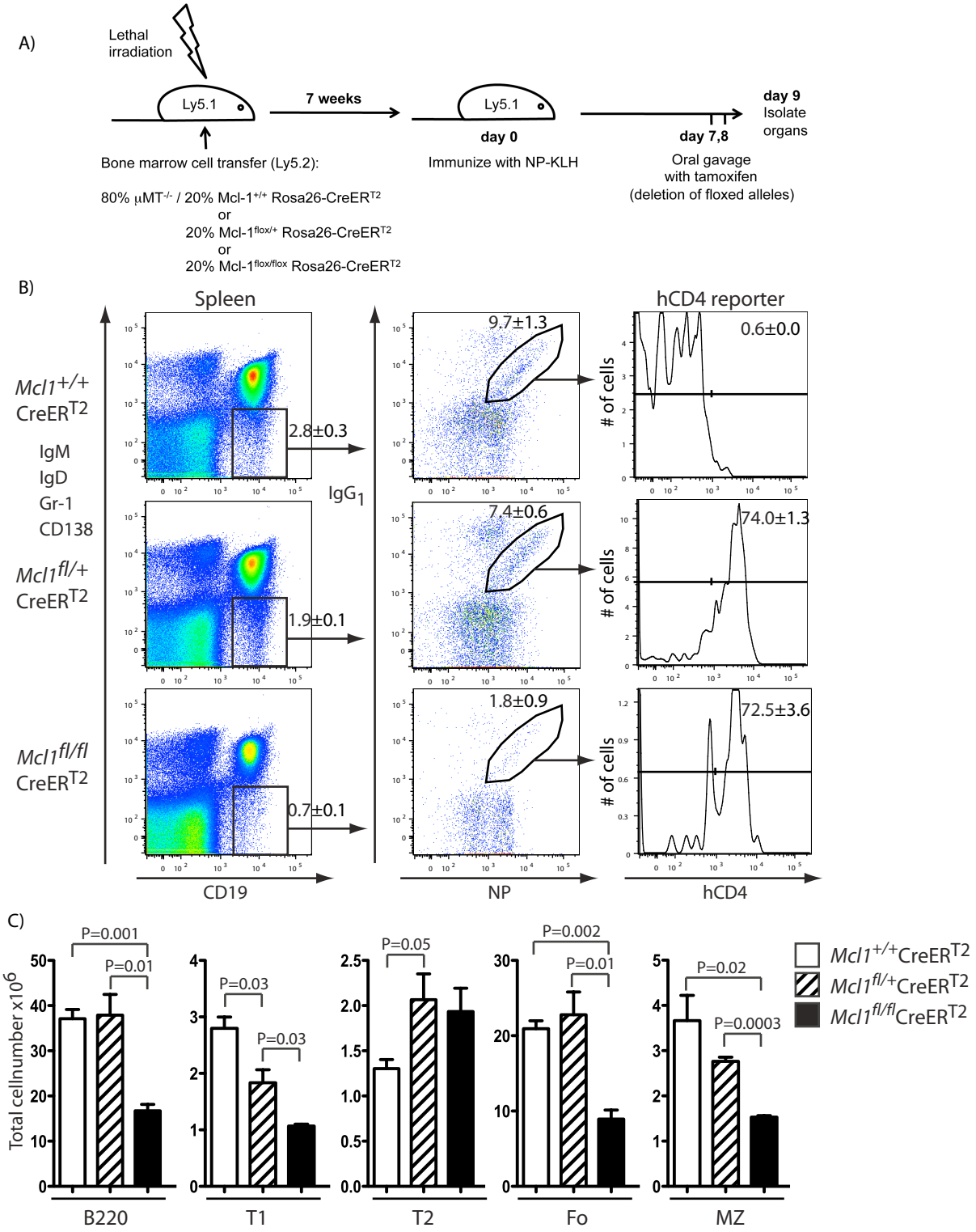


**Fig. S13.** Induced deletion of *Mcl1* leads to loss of $NP^+IgG_1^+$ B cells during an immune response. (**A**) Irradiated C57BL/6-Ly5.1 mice were reconstituted with 80% B cell deficient (μMT) bone marrow plus 20% bone marrow from *Mcl1*$^{+/+}$CreER$^{T2}$, *Mcl1*$^{fl/+}$CreER$^{T2}$, or *Mcl1*$^{fl/fl}$CreER$^{T2}$. In the resultant chimeras, all B cells contained CreER$^{T2}$, expressed from the *Rosa26* locus, and were either resistant (*Mcl1*$^{+/+}$) or sensitive to *Mcl1* deletion on one (*Mcl1*$^{fl/+}$) or both (*Mcl1*$^{fl/fl}$) alleles. (**B**) Flow cytometric analysis of antigen-specific B cells persisting after induced deletion of *Mcl1*. Seven days after intrapertioneal immunization with NP-KLH in alum, mice were treated on two successive days with Tamoxifen to induce Cre activity and their spleens analysed for the frequency of isotype switched ($IgM^-IgD^-Gr\text{-}1^-CD138^-B220^+$) B cells that were $NP^+IgG_1^+$. The amount of hCD4– indicative of *Mcl1* deletion– expressed on the remaining $NP^+IgG_1^+$ cells was determined. (**C**) Total numbers of splenic $B220^+$ cells, $CD23^-IgM^+CD21^{int}$ transitional 1 (T1) cells, $CD23^+IgM^{hi}CD21^{hi}$ transitional 2 (T2) cells, $CD23^+IgM^{int}CD21^{int}$ follicular (Fo) cells and $CD23^-IgM^+CD21^{hi}$ marginal zone (MZ) cells in naive mice. Significant differences, calculated using Student's T-test, are indicated. Data are from 3 mice per group.

Supplementary figure 14

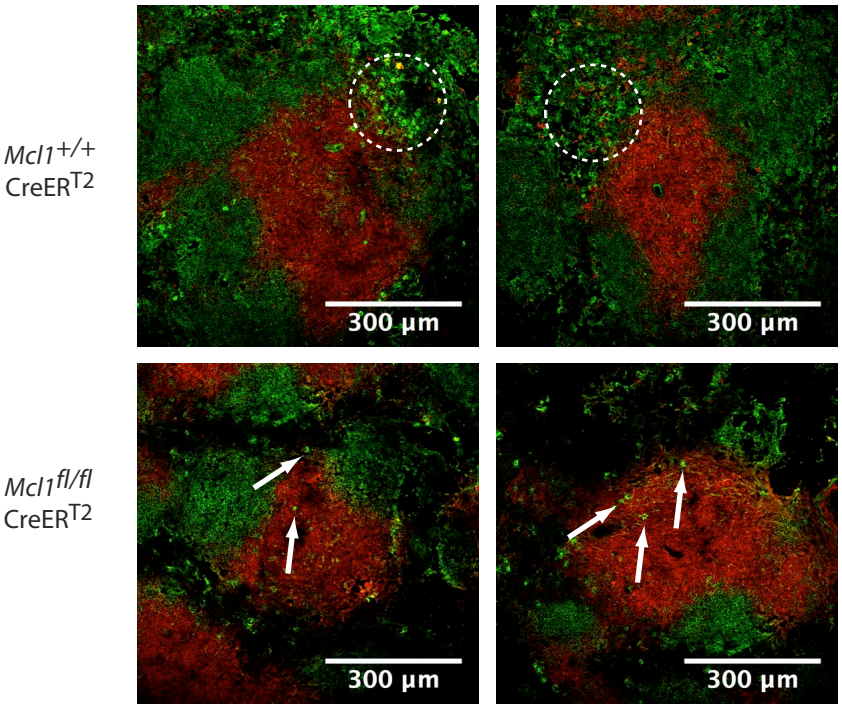


**Fig. S14.** Induced deletion of *Mcl1* leads to reduction in IgM$^{+}$ plasma blasts.
Irradiated C57BL/6-Ly5.1 mice were reconstituted with 80% B cell deficient (µMT) bone marrow plus 20% bone marrow from *Mcl1*$^{+/+}$CreER$^{T2}$, *Mcl1*$^{fl/+}$CreER$^{T2}$, or *Mcl1*$^{fl/fl}$CreER$^{T2}$. In the resultant chimeras, all B cells contained CreER$^{T2}$, expressed from the *Rosa26* locus, and were either resistant (*Mcl1*$^{+/+}$) or sensitive to *Mcl1* deletion on one (*Mcl1*$^{fl/+}$) or both (*Mcl1*$^{fl/fl}$) alleles. Seven days after intrapertioneal immunization with NP-KLH in alum, mice were treated on two successive days with Tamoxifen to induce Cre activity. Frozen sections of spleens from the indicated strains were stained with anti-IgM (green) and anti-CD3 (red). IgM plasma blasts are indicated by dotted circles and arrows. Original magnification x 20 with scale indicated.